Macromolecules

Article

pubs.acs.org/Macromolecules

Chain Conformation near the Buried Interface in Nanoparticle-Stabilized Polymer Thin Films

Deborah A. Barkley,[†] Naisheng Jiang,[‡] Mani Sen,[‡] Maya K. Endoh,[‡] Jonathan G. Rudick,[†] Tadanori Koga,*[,†,‡] Yugang Zhang,[§] Oleg Gang,[∥,⊥] Guangcui Yuan,[#] Sushil K. Satija,[#] Daisuke Kawaguchi,[%] Keiji Tanaka,[&] and Alamgir Karim[$]

[†]Department of Chemistry and [‡]Department of Materials Science and Chemical Engineering, Stony Brook University, Stony Brook, New York 11794, United States

[§]National Synchrotron Light Source II and [∥]Center for Functional Nanomaterials, Brookhaven National Lab, Upton, New York 11973, United States

[⊥]Department of Chemical Engineering and Applied Physics and Applied Mathematics, Columbia University, New York, New York 10027, United States

[#]Center for Neutron Research, National Institute of Standards and Technology, Gaithersburg, Maryland 20899, United States

[%]Education Center for Global Leaders in Molecular Systems for Devices and [&]Department of Applied Chemistry, Faculty of Engineering, Kyushu University, Fukuoka 819-0395, Japan

[$]College of Polymer Science and Polymer Engineering, The University of Akron, Akron, Ohio 44325-0301, United States

Supporting Information

ABSTRACT: It is known that when nanoparticles are added to polymer thin films, they often migrate to the film−substrate interface and form an "immobile interfacial layer", which is believed to be the mechanism behind dewetting suppression. We here report a new mechanism of dewetting suppression from the structural aspect of polymer chains accommodated at the film−substrate interface. Dodecanethiol-functionalized gold (Au) nanoparticles embedded in relatively low molecular weight PS thin films prepared on silicon (Si) substrates were used as a model. We mimicked the previously reported conditions, where the nanoparticles preferentially migrate to the substrate, and successfully stabilized the PS thin films via thermal annealing. A suite of surface-sensitive techniques including atomic force microscopy, grazing incidence small-angle X-ray scattering, X-ray/neutron reflectivity, and sum frequency generation spectroscopy in conjunction with the established solvent leaching process enabled us to unveil the polymer chain conformation and the dispersion structure of the nanoparticles at the film−substrate interface. The results evidenced that thermal annealing promotes irreversible polymer adsorption onto the substrate surface along with the migration of the nanoparticles. In addition, we found that the migration of the nanoparticles causes the changes in the conformations and interfacial orientations of the adsorbed polymer chains compared to those of the adsorbed polymer chains formed in the nanoparticle-free PS thin film. The resultant interfacial polymer structure allows for the interpenetration between free chains and the adsorbed chains, thereby stabilizing the thin film.

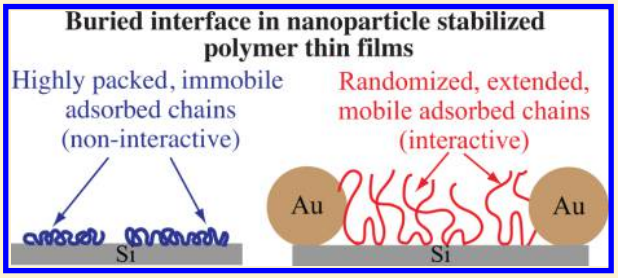

I. INTRODUCTION

Owing to strong demands for newly emerging polymer-based nanotechnologies such as photovoltaic cells, semiconductor chips, and biosensors,[1−3] many sophisticated devices are now moving toward nanometer scales, while maintaining exceptional performance capabilities. The key for breakthroughs in such advanced polymer-based technologies is the formation of a stable solid−polymer melt (SPM) interface which determines the stability/reliability[4] and properties/functionalities[5,6] of these materials. However, the study and understanding of the SPM interface is a very challenging task because the length scale of the SPM interface is typically limited to a few nanometers or less and the interface is always in contact with the thicker part of the polymer and/or solid material.

Herein, we focus on one of the long-standing questions at the SPM interface of nanoparticle-stabilized polymer thin films. It is known that the inclusion of a very small amount of nanoparticles stabilizes ultrathin polymer films against dewetting upon thermal annealing. Nanoparticles often migrate to the film−substrate interface[7−22] and form a "diffused immobile interfacial layer".[7,16,18,22,23] The particle migration is attributed

Received: June 6, 2017
Revised: September 7, 2017
Published: September 26, 2017

DOI: 10.1021/acs.macromol.7b01187
Macromolecules 2017, 50, 7657−7665

to an entropy-driven mechanism known as depletion attraction.[14,24−27] Krishnan and co-workers showed that the loss in the translational entropy as well as the enthalpy due to particle mixing is offset by the gain in the conformational entropy of polymer chains, as they are dislocated from the substrate due to the particle migration.[15] It is believed that the migration alters the surface energy and consequently the wetting property of the substrate, resulting in a change in the nature of the effective interaction between the film and substrate.[19]

On the other hand, we recently evidenced that polymer chains adsorbed onto solids play a crucial role in thermal stability of single PS thin films (without the inclusion of nanoparticles) on Si substrates.[28] There is growing evidence to support that polymer melt chains irreversibly adsorb even onto weakly attractive planar solid surfaces.[28−42] Recently, we revealed that the adsorbed layer consist of two different chain conformations regardless of the magnitude of attractive solid−segment interactions:[35,36] During adsorption of polymer chains, early arriving chains lie flat on a solid ("flattened chains") and improve the segmental packing during an equilibrium pathway to promote continued adsorption of additional chain segments.[43] On the other hand, late arriving chains form bridges jointing up nearby empty sites available, resulting in "loosely adsorbed chains". The resultant two different chain conformations are analogous to those formed via polymer adsorption from a dilute solution.[44,45] The PS thin films (20 nm in thickness) annealed at a high temperature above the glass transition temperature showed a dewetting-to-wetting transition controlled by molecular weight. We elucidated that the PS films were stable when the loosely adsorbed polymer chains were formed on the substrates; conversely, the lone flattened chains were noninteractive even with chemically identical free polymer chains, resulting in autophobic dewetting at the flattened polymer−free polymer interface.[28] Thus, the interfacial polymer conformation, which has until now been paid little attention, is of importance for controlling the wetting property.

In this paper, we use two different molecular weights of monodisperse polystyrene (PS, M_w = 30 and 50 kDa) and dodecanethiol-functionalized gold (Au) nanoparticles as a model system and investigate the role of the chain conformation at the SPM interface in thermal stability of the model polymer/nanoparticle blend films. As mentioned above, the nanoparticle-free PS thin films composed of these two relatively low M_w PS dewet at the flattened polymer−free polymer interface. By tuning the interfacial energetics, we mimicked the previously reported conditions, where the nanoparticles preferentially migrate to the substrate,[7−22] and could successfully stabilize the PS thin films. Detailed characterizations at the SPM interface of the blend films are intriguing to show significant changes in the microscopic conformations of the flattened chains that are responsible for dewetting of the nanoparticle-free PS thin films: the flattened chains at the SPM interface of the blend films are extended in the direction normal to the film surface, and the orientations of the main chains and the phenyl groups become randomized against the substrate surface. In addition, the randomized and extended flattened chain (we hereafter assign them as "RE flattened chains") is no longer immobile, as opposed to the prevailing concept of the "diffused immobile interfacial layer"[7,16,18,22,23] at the SPM interface of nanoparticle-stabilized polymer thin films. The experimental data further indicate that the emergence of the RE flattened chains is associated with the surface migration of the nanoparticles that creates additional "nanoconfinement" on the flattened chains in the direction parallel to the substrate surface. Consequently, the RE flattened chains allow for the interpenetration of free chains in the bulk of the film, resulting in a stable adsorbed polymer−free polymer interface. The present understanding can directly impact the practical uses of this class of materials, facilitating breakthroughs in advanced and traditional polymer thin film based technologies.

II. RESULTS

Monodisperse PS (M_w = 30 and 50 kDa, M_w/M_n < 1.1) and dodecanethiol-functionalized Au nanoparticles with the average diameter of 5.8 nm (the core Au diameter of 2.8 nm and the shell thickness of 1.5 nm) were used. Hereafter we assign PS (M_w = 30 kDa) and PS (M_w = 50 kDa) as PS30k and PS50k, respectively. Solutions of the PS were first prepared in toluene. The different Au nanoparticle solutions with concentrations (ϕ_{Au}) varying from 0 to 0.25 vol % (volume of the particle/volume of the polymer) were then added to the PS solutions, which were further sonicated for 30 min to disperse the Au nanoparticles. To study the effect of the Au nanoparticles on film stability, we prepared 20 nm thick PS/Au blend films on cleaned Si substrates covered with a native SiO_x layer of 2.4 nm in thickness. The detailed sample preparation procedures including cleaning of the substrates are described in the Experimental Section.

Karim and co-workers recently proposed a new parameter, $E_p = \gamma_{S-P} - \gamma_{S-N}$, where γ_{S-P} and γ_{S-N} are the interfacial energies between the substrate and polymer and between the substrate and nanoparticles, respectively, to evaluate how the relative magnitude of the interfacial energies influences the migration of the particles and subsequently suppression of dewetting.[22] On the basis of systematic experiments of dewetting of PS thin films containing fullerene nanoparticles, they demonstrated that a higher positive value of E_p implies preferred migration of nanoparticles toward the substrate surface. To discuss the E_p value for the present system, we obtained the surface tension of the Au nanoparticles by spin-coating them onto a cleaned Si substrate and then measured the contact angles of three liquids (water, glycerol, and 1,4-butanediol) on the Au monolayer. Based on the results (Supporting Information), $E_p > 0$ was calculated for the Si substrate such that the Au nanoparticles preferentially migrate toward the substrate. The PS/Au blend films were then annealed in a vacuum of 10^{-3} Torr at 150 °C for a prolonged period of time up to 300 h. The PS/Au thin films were subsequently quenched to room temperature to check the film stability using optical microscopy (OM).

Figure 1 shows the OM images of the PS30k/Au thin films. As 0.05−0.25% of the Au nanoparticles were added to the PS, partial dewetting was observed (Figure 1b−d). Especially, at ϕ_{Au} = 0.25% loading, the dewetting was significantly suppressed (Figure 1d) even after t_{an} = 300 h annealing, which is qualitatively consistent with previous findings.[22] We confirmed that dewetting suppression of the PS50k/Au thin films (20 nm in thickness) was also achieved by adding similar amounts of the Au particles to the PS50k matrix.

We then focused on the interfacial polymer structure near the substrate. Guiselin[46] proposed the experimental procedure to unveil an irreversibly adsorbed polymer layer buried under the polymer melts. In this method, one has to equilibrate the melt against a solid wall; the unadsorbed chains can then be

DOI: 10.1021/acs.macromol.7b01187
Macromolecules 2017, 50, 7657−7665

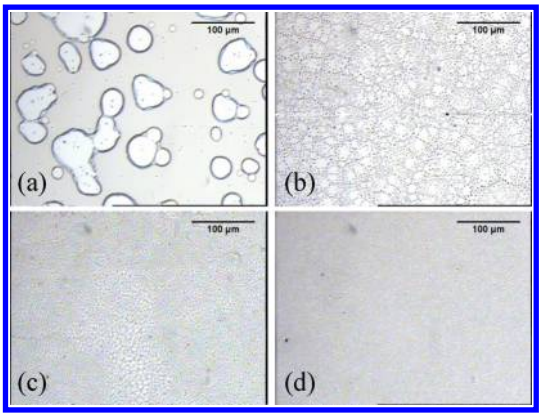

Figure 1. Optical microscopic (OM) images of the PS30k/Au 20 nm thick films after annealing 18 h at 150 °C: (a) pure PS, (b) 0.05% Au; (c) 0.10% Au; (d) 0.25% Au. The scale bars correspond to 100 μm.

removed by a good solvent, while the adsorbed chains are assumed to maintain the same conformation due to the irreversible freezing they experience through the many solid–segment contacts. Despite experimental difficulties, several research groups have proved that Guiselin approach is practical for various homopolymers[29,30,32–42] (known as a "Guiselin brush").[46] We previously reported that for PS30k and PS50k the densely packed flattened chains with thicknesses of about 2 nm mainly grow on the Si substrate via the equilibrium pathway.[35,36] They prevent the penetration of free (unadsorbed) molecules since the cost for stretching the molecules is always higher than a gain in translational entropy,[47] prompting dewetting of the thin polymer films at the adsorbed polymer–free polymer interface instead of the solid–polymer interface.[28] Motivated by these results, we rinsed the annealed PS50k/Au thin films with toluene (a good solvent for PS) thoroughly and dried them at 150 °C under vacuum.

Figure 2a,b shows representative atomic force microscopy (AFM) images of the PS/Au (0.25%) and counterpart pure PS residual (flattened) layers after annealing at 150 °C for t_{an} = 72 h and subsequent thorough leaching with solvent to remove unadsorbed chains. All the residual layers which remained after rinsing were further dried at 150 °C for 24 h. We independently confirmed the presence of Au (and PS) on the substrate using XPS experiments (Figure S1) and grazing- incidence small-angle X-ray scattering (GISAXS, Figure 2f). The AFM results show that the solid surface was entirely covered with the PS chains (see Figure 2a) for the PS/Au flattened layer, while the substrate was partly covered with the polymer when the Au nanoparticles were not embedded (Figure 2b). Figure 2a also indicates the dispersion of the individual Au nanoparticles within the local area. The dimple structures of the PS flattened layer with the average width of several tens of nanometers and the average height of about 2 nm (Figure 2e) were formed on the substrate surface, as previously reported.[28,36] The average spacing between the dimple structures was estimated to be 100 nm (Figure 2e). We also found larger Au clusters with the average size of 60 nm and the average distance between the clusters of about 500 nm under enlarged AFM scan (Supporting Information). As discussed below, the large clusters would have only a minimal effect on the chain conformations. It was found that the average RMS roughness of the well-dispersed Au/polymer regions is independent of the Au concentrations with the value of 0.21 ± 0.05 nm (Supporting Information). Based on the AFM projected area,

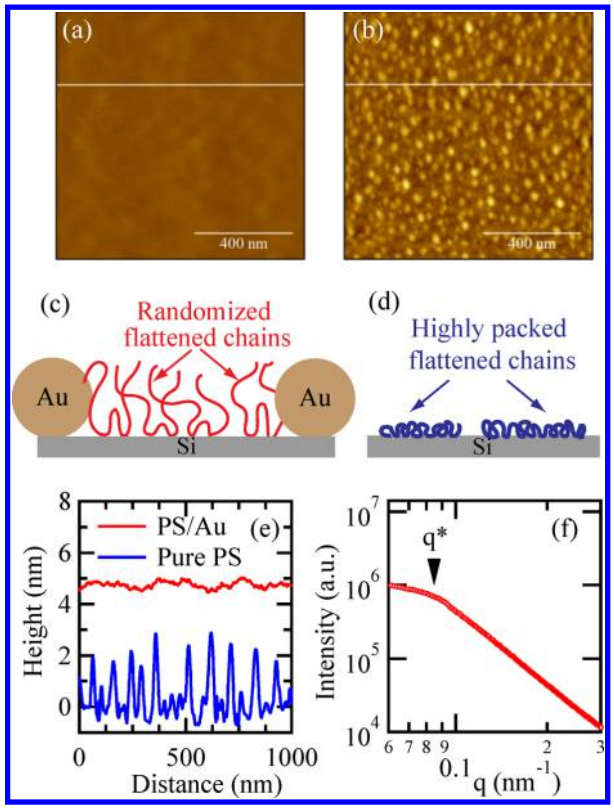

Figure 2. AFM height images of (a) the PS50k/Au (0.25%) flattened layer and (b) the pure PS flattened layer. The height scales of both images are 0–10 nm. Note that the AFM images are focused on the well-dispersed Au/polymer regions to avoid the disturbance of the large Au clusters on the morphology of the flattened chains, as shown in Figure S2. Schematic views of the two different types of the chain conformations on the substrate are shown in (c) (with Au) and (d) (without Au). The circle in (c) represents the overall size of the individual Au particle including the shell part. The corresponding height (from the SiO_x surface) profiles along the white lines in (a) and (b) are plotted in (e). (f) GISAXS data for the PS50k/Au (0.25%) flattened layer. q^* corresponds to the peak position.

the volume fraction of the large clusters in the PS50k/Au (0.25%) flattened layer was approximated to be 0.7% (Supporting Information). Hence, it is clear that a significant amount of the nanoparticles as a whole migrates to the substrate surface, in accordance with the entropic-push hypothesis.[14,15,22,24–27] It should be noted that as discussed above and later, the individual nanoparticles and some portions of the large clusters are embedded into the flattened layer. Therefore, the actual concentration of the nanoparticles in the flattened layer should be larger than the estimated one.

Figure 3 shows representative XR profiles for the PS50k (top) and PS50k/Au (0.05%) flattened layers (bottom) layers prepared by annealing at 150 °C for t_{an} = 72 h and subsequent thorough leaching with solvent to remove unadsorbed chains. All the residual layers were further dried at 150 °C for 24 h. We utilized a three-layer model (a Si substrate, a SiO_x layer, and a PS layer) for the XR fitting. The details of the XR fitting have been described elsewhere.[35,36] The best fits (the black solid lines) to the XR profile were calculated based on the dispersion (δ) profiles shown in the inset of Figure 3. The thickness and the dispersion value (which is proportional to the density of a film) of the pure PS flattened layer were determined to be 1.9 nm and $\delta = 0.68 \times 10^{-6}$, respectively, while the thickness and

DOI: 10.1021/acs.macromol.7b01187
Macromolecules 2017, 50, 7657–7665

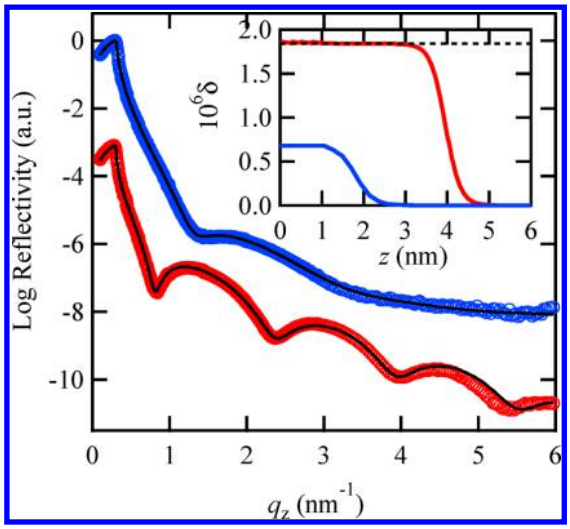

Figure 3. XR of the PS50k (indicated in blue) and PS50k/Au (0.05%) residual layers (indicated in red). The solid lines are the calculated RF based on the density profiles shown in the inset: the PS50k flattened layer (blue) and the PS50k/Au (0.05%) (red) flattened layer.

dispersion value of the PS/Au (0.05%) flattened layer were 4.0 nm and $\delta = 1.84 \times 10^{-6}$. Note that the bulk δ value of PS with the X-ray energy (11.25 keV) is $\delta_{bulk} = 1.84 \times 10^{-6}$. The lower δ value of the nanoparticle-free PS flattened layer corresponds to the formation of the inhomogeneous layer (see Figure 2b).

Figure 4 shows the time evolution of the flattened layer measured by XR. From the figure we can see that the thickness

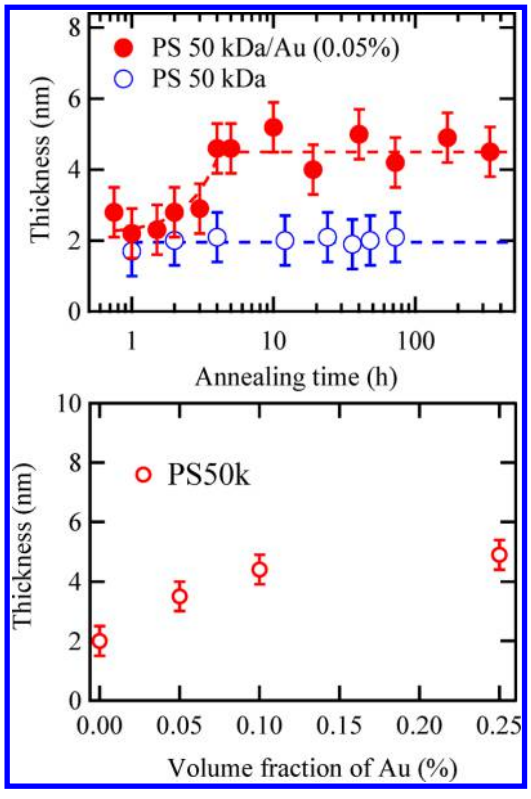

Figure 4. (a) Time evolution of the PS50k/Au (0.05%) and pure PS50k flattened layers as a function of t_{an}. (b) Concentration dependence of the PS/Au residual layers after annealing at 150 °C for 96 h.

of the flattened chains is nearly identical to that of the counterpart particle-free PS flattened layer at $t_{an} < 2$ h. However, the chains grow further and the thickness reaches a plateau value of 4.6 ± 0.5 nm at $t_{an} > 4$ h. We confirmed that dewetting seen in Figure 1a becomes visible after annealing the pure PS thin film at 150 °C for more than about 4 h. Hence, it is indicative that the formation of the extended flattened chains is correlated with the time scale for dewetting suppression.

During the course of thermal annealing, a large number of the nanoparticles migrate to the substrate surface even before the film has ruptured on the basis of the concept of $E_p > 0$.[22] As mentioned above, these nanoparticles then push unadsorbed polymer chains away from the solid wall. In contrast, the (nonequilibrium) PS flattened chains emerge under solution conditions (during spin-coating) rather than under melt conditions,[29,48] and the highly packed chain conformation develops after several hours of annealing at 150 °C in the pure PS50k flattened layer.[36] As clarified previously,[42] increasing the number of surface-segmental contacts is the driving force for the equilibrium flattening process to overcome the conformational entropy loss in the total free energy (Figure 2d). Hence, this increase in the thickness of the PS/Au flattened layer suggests that the local packing of the flattened chains via the equilibration pathway on the substrate is hindered by the presence of the Au nanoparticles. It should also be emphasized that the thickness of the RE flattened chains increases with increasing Au concentration (at least up to $\phi_{Au} = 0.25$ (Figure 4b), which is consistent with recent molecular dynamics simulation results.[49]

In order to confirm this structural hypothesis, we investigated the local chain conformations of the flattened chains using sum frequency generation spectroscopy (SFG), which takes advantage of the fact that generation of an SFG photon is forbidden in the centrosymmetric bulk but is nonzero at interfaces where inversion symmetry is broken.[50,51] Since our previous results[42] showed that the majority of the SFG signal under ssp (SFG/s; visible/s; and IR/p) polarization from the PS thin film is attributed to the flattened chains, we measured the SFG signal from the 20 nm thick PS/Au thin film prepared on a quartz prism directly. Figure 5 shows the SFG spectrum from the PS50k/Au (0.05%) film annealed at 150 °C for 96 h. As a control, we also plotted the SFG spectrum from the counterpart pure PS thin film annealed at 150 °C for $t_{an} = 96$ h where we can see three peaks at 2906, 3030, and 3060 cm^{-1}, which are attributed to the contributions from the C−H

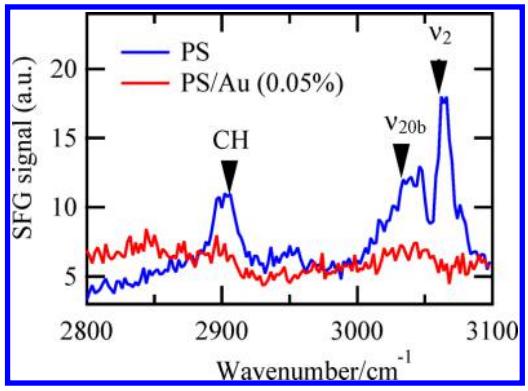

Figure 5. SFG spectra with the *ssp* polarization combination for the PS50k/Au (0.05%) and pure PS films annealed at 150 °C for $t_{an} = 96$ h.

DOI: 10.1021/acs.macromol.7b01187
Macromolecules 2017, 50, 7657−7665

stretching vibration of methyne (CH) groups,[52] the ν_{20b} vibrational mode, and the ν_2 vibrational mode of phenyl rings, respectively.[53] These peaks in the pure PS thin film indicate that both the main chains and the phenyl groups have nonrandom interfacial orientations: the backbone chains are directed toward the weakly interactive quartz substrate to increase the number of the solid/segment contacts,[29,37] while the preferential interfacial orientation of the phenyl ring is attributed to the polar nature of the silanol groups on the substrate as well as the interaction between the Π electron cloud of the phenyl ring and a surface hydroxyl (OH) group of the quartz surface.[54] It should be noted that we previously reported that the phenyl rings of much longer PS (M_w = 290 kDa) chains are randomized under the same thermal annealing condition.[42] This opposing finding in the present SFG data is attributed to the fact that the effect of an elongated chain conformation along the lateral direction of the substrate surface increases with increasing a chain length in such a very confined geometry (~2 nm in thickness), preventing the compact chain packing of the longer chain as a whole.[55] Intriguingly, when the Au nanoparticles migrate to the substrate, none of these peaks appear, implying that the chain orientations have become randomized ("randomized flattened" (RF) chains) due to the segregation structure of the Au nanoparticles during the thermal annealing process.

In order to further shed light on the structures of the Au nanoparticles in the flattened layer, GISAXS was utilized. Since Au has the inherent strong X-ray contrast compared to the polymer, the structure of the nanoparticles (that was "invisible" to AFM) embedded in the flattened layer can be identified by GISAXS. As shown in Figure 2f, the scattering profile from the PS50k/Au (0.25%) flattened layer clearly shows the peak that corresponds to the interparticle (or cluster) spacing of nearly 70 nm ($\approx 2\pi/q^*$). Hence, the migration of the Au nanoparticles induces additional "confinement" on the polymer chains in the direction parallel to the film. It is thus anticipated that this nanoconfinement, whose length scale is comparable to the size of the dimple structures of the nanoparticle-free PS flattened layer (Figure 2b), prevents the zipping down (equilibration) process of the nonequilibrium flattened chains.[35,36,42] As a consequence, the resultant chain conformation confined between the Au clusters is not highly packed but is expanded in the direction normal to the film to retain the bulk density of the film (Figure 2c). It should be noted that Figure 2c illustrates this nanoconfinement effect on the conformation of the flattened chains by contrasting with the nanoparticle-free PS flattened chains (Figure 2d).

III. DISCUSSION

Having the structural origin of the RF chains, we now discuss the possible mechanism of how the RF chains stabilize the polymer−polymer interface where dewetting of the counterpart PS thin films initiates and develops holes.[28] For this purpose, we mimicked the single PS50k/Au layer by utilizing split layers composed of a deuterated PS (dPS, M_w = 333 kDa, M_w/M_n = 1.05, Polymer Source) overlayer (without Au) on top of the PS50k/Au (0.25%) RF chains, while the total thickness of the split layer was fixed to about 20 nm. The PS50k/Au (0.25%) flattened layer was independently prepared on Si, and the dPS overlayer (about 20 nm thick) was then floated on top from deionized water. The interpenetration process at $T > T_g$ was then examined by neutron reflectivity (NR). The NR data corrected for the background scattering (Figure 6) were

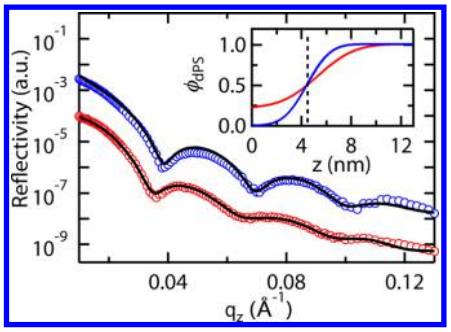

Figure 6. NR results for the bilayers of the PS50k/Au (0.25%) flattened layer and the top d-PS film: t_{an} = 0 h (blue); t_{an} = 171 h (red) at 150 °C. The solid lines are the best-fits to the data based on the volume fraction profiles of dPS (ϕ_{dPS}) shown in the inset: t_{an} = 0 h (blue); t_{an} = 171 h (red) at 150 °C.

analyzed by comparing the observed reflectivity curves with the calculated ones based on model scattering length density profiles composed of Si, SiO_x, the hPS/Au flattened layer, and the dPS overlayer. As shown in the inset of Figure 6, the dPS chains interpenetrate into the flattened chains (i.e., $\phi_{dPS}(z=0)$ = 0.2), increasing in this way the entropy of the free chains and further resulting in the broadening of the free polymer-adsorbed polymer interface. Note that the root-mean-square interfacial roughness (σ) between the layers remained nearly unchanged (σ = 5.5 ± 0.5 nm) up to annealing time of 171 h (Supporting Information). On the other hand, control NR experiments for a bilayer composed of the dPS 20 nm thick overlayer on top of the nanoparticle-free PS50K flattened layer demonstrated that the nanoparticle-free flattened chains do not allow penetration of the free d-PS chains even at $T \gg T_g$, resulting in a sharp free polymer-adsorbed polymer interface (σ = 1.1 ± 0.5 nm) (Supporting Information). This causes dewetting at the flattened polymer−free polymer interface,[28] as seen in Figure 1b.

Using molecular simulations, Luo and Gersappe[56] showed that suppression of dewetting of nanofilled polymer thin films on a substrate is due to the immobility of the polymer chains in the nanoparticle-rich layer. Hence, their hypothesis may not apply to our experimental results. On the other hand, nanoparticle segregation to the polymer−substrate interface could conceivably modulate slippage of the film on its substrate.[57] However, any amount of slippage greatly accelerates the dynamics of instability and hole growth, whereas just the reverse is observed here.[19] Thus, slippage is not a causative factor in an explanation of the present results.

Rather, this behavior bears similarity to that of a wetting to dewetting transition at the interface between a brush and a melt of chemically identical polymer chains. Leibler and co-workers[58] demonstrated that brush chains undergo the transition from wet brush to dry brush as the grafting density increases, when the ratio of the polymerization indices of the free (P) and brush chains (N) are equal to or greater than 1. While the grafting density of a Guiselin brush (σ_T), which is defined as $\sigma_T = ((n_{tail} + 2n_{loop}))/(L_xL_y)$, where L_xL_y is the area of the substrate and n_{tail} and n_{loop} are the number of tails and loops of the adsorbed polymers, respectively,[43] is difficult to quantify experimentally the aforementioned SFG results support the decrease in the number of the substrate−segmental contacts of the flattened chains in the presence of the Au nanoparticles. Hence, we may conclude that the change in the effective grafting density of the flattened chains associated with

DOI: 10.1021/acs.macromol.7b01187
Macromolecules 2017, 50, 7657−7665

the surface migrating nanoparticles is the origin of the nanoparticle-stabilized polymer thin films. At the same time, the NR results indicate the interdigitation of the RF chains into the d-PS melt chains. These RF chains would play a role as "connectors", which effectively promote adhesion of a polymer thin film on a solid predicted by Raphaël and de Gennes[59] and experimentally verified by Reiter and co-workers.[60−62] Further experiments are needed to reveal the structure−property relationship at the polymer−polymer interface.

Finally, we discuss the morphology of the large Au clusters in the flattened layer. Kim and O'Shaughnessy discussed aggregated structures of brush-"insoluble" nanoparticles bulged into a polymer brush, depending on the strength of nanoparticle−polymer brush interactions and the concentration of the nanoparticles based on molecular dynamics simulations.[63] We extend this concept to our flattened layer (i.e., polydisperse brushes).[46] At high concentrations, such aggregates form a baguette shape of clusters at the polymer/air interface on the basis of the spreading coefficient and the entry coefficient. The entry coefficient, E_d, is defined as $E_d = \gamma_{PS-Air} + \gamma_{PS-Au} - \gamma_{Au-Air}$, where γ_{PS-Air} is the surface tension between PS and air, γ_{PS-Au} is the surface tension between PS and Au nanoparticles, and γ_{Au-Air} is the surface tension between Au nanoparticles and air. On the other hand, the spreading coefficient is defined as $S_d = \gamma_{PS-Air} + \gamma_{PS-Au} - \gamma_{Au-Air}$. All the numbers used in this study are listed in the Supporting Information. We calculated $E_d = 90.98 + 1.12 - 89.72 = 1.48$ mJ/m^2 and $S_d = 90.98 - 1.12 - 89.72 = -0.76$ mJ/m^2. Hence, droplet entry into the polymer−air interface is favored since $E_d > 0$ and the growth of the aggregates in the lateral direction is arrested ($S_d < 0$), displaying a characteristic size of the aggregates. Consequently, we conclude that the nanoparticles form clusters and the clusters enter into the flattened chains, forming the so-called baguette-shaped cluster[63] and thereby preventing the clusters from washing away during the intensive solvent leaching process.

IV. CONCLUSION

In summary, we describe a new mechanism of nanoparticle-stabilized polymer thin films using model polymer nanocomposite thin films. The concurrent phenomena that led to this mechanism are the surface migration of the nanoparticles and polymer adsorption, which both occur at the polymer melt−solid interface during thermal annealing. We have found that the conformation of the flattened chains is randomized and expanded in the direction normal to the film surface due to the limited space in the lateral direction of the substrate where the nanoparticles migrate toward and occupy. The randomized and loosened flattened chains (i.e., the RF chains) are mobile and penetrate into the bulk of the film (acting as connectors) or allow for penetration of the free chains in the bulk of the film, broadening the interfacial width between the free polymer−adsorbed polymer interface and thus improve adhesion at the SPM interface. To further provide the general principle of the mechanism of nanoparticle-stabilized polymer thin films, we will focus on the following parameters: film thickness,[64,65] the size of nanoparticles,[56] the ratio of R_g of the polymer to the nanoparticle size,[12] the ratio of the particle diameter to the monomer diameter,[14] interfacial interactions,[22] and the interparticles (or intercluster) spacing of the nanoparticles on the substrate. Moreover, it would be of interest to examine the effect of the T_g of the PS adsorbed layer, which was previously reported to be considerably higher than the bulk T_g,[40] on the dewetting suppression.

V. EXPERIMENTAL SECTION

Materials. Dodecanethiol-functionalized gold nanoparticles with average diameter size of 2.8 nm were obtained via a solution phase reaction.[66] The purposes of dodecanethiol functionalization are (i) to stabilize the gold cores against aggregation and (ii) to prevent direct adsorption of polymer segments to the nanoparticle cores.[67] The nanoparticle core size was determined by small-angle X-ray scattering (SAXS). With an *all-trans* conformation, the dodecanethiol surfactant (shell) is ∼1.5 nm long, resulting in a particle with 5.8 nm diameter in total (grafting density is 1 chain per 0.2 nm^2).[68,69] The nanoparticles were stored as a 1 wt % solution in toluene. Sonication of the nanoparticle toluene solution for 30 min resulted in dispersion of the nanoparticles in solution on the basis of solution SAXS experiments. PS30k and PS50k were purchased from Pressure Chemicals Co. Deuterated PS (M_w = 333 kDa) was purchased from Polymer Source Inc. Toluene (>99.5%) and chloroform (≥99.8%) were purchased from Sigma-Aldrich. PS was dissolved in toluene. These solutions were added to solutions of the gold nanoparticles. Note that the gold nanoparticles only interact weakly with PS chains due to the presence of the dodecanethiol shell based on previous results.[32,70,71] The combined nanoparticle and polymer solutions were sonicated for 30 min to produce homogeneous solutions. The polymer nanoparticle solutions were used immediately to spin-cast films.

Silicon (Si) wafers were cleaned by a modified Shirake technique.[72] The wafers were cleaned by heating, uncovered, without stirring, for 20 min at 150 °C in aqueous hydrogen peroxide and ammonium hydroxide and rinsing with deionized water, followed by heating for 20 min in aqueous hydrogen peroxide and concentrated sulfuric acid. *Caution: solutions of hydrogen peroxide and sulfuric acid are highly corrosive to skin and eyes and also pose a risk of explosion when in contact with organic materials. Extreme care must be used.* The wafers were then rinsed five times with distilled water. To prepare the samples for dewetting, we used the exact same protocols for all Si wafer cleaning to avoid possible differences in the surface chemistry of the oxide layer that may affect dewetting behavior of PS and PS/Au films.[73] By using X-ray reflectivity, we confirmed that the native SiO_x layer after the piranha solution cleaning had a thickness of d_{SiOx} = 2.4 nm on the Si with a surface roughness of less than 0.5 nm.[28] The polymer thin films were created by spin-casting from PS toluene solutions or PS/Au solutions for 30 s at 2500 rpm. The spin-cast polymer thin films were annealed at 150 °C in a vacuum oven at 10^{-3} Torr for prolonged annealing times of up to 300 h. The adsorbed layers were revealed by rinsing away the unadsorbed polymer with a good solvent, toluene, according to the previously reported protocol.[28,30,34,36]

Techniques. Surface morphologies of the flattened layers were studied using atomic force microscopy (AFM) (Veeco Multimode V) and atomic force microscopy (AFM) (Agilent 5500 AFM/SPM, Keysight Technologies Inc., USA). A standard tapping mode was conducted in air using a cantilever with a spring constant of about 40 N/m and a resonant frequency of about 300 kHz. The scan rate was 0.5−1 lines/s with a scanning density of 512 lines/frame.

Optical microscope (OM) measurements were conducted by using reflective light under an Olympus BHT microscope equipped with a differential interference contrast attachment for incident light after Nomarski (NIC Model). OM images were captured by a digital camera at room temperature.

X-ray reflectivity (XR) was performed at the Cornell High Energy Synchrotron Source (CHESS) beamline G2. The experiments were performed under vacuum (approximately 10^{-4}−10^{-5} Torr). The specular reflectivity was measured as a function of the scattering vector, $q = 4\pi \sin\theta/\lambda$, using an X-ray wavelength of 0.1102 nm (which is equivalent to the X-ray energy of 11.25 keV). The XR data were fit by using a standard multilayer fitting routine for a dispersion value (δ in the X-ray refractive index) in conjunction with a Fourier transformation (FT) method, a powerful tool to obtain detailed structures for low X-ray contrast polymer multilayers.[74,75] The δ values

DOI: 10.1021/acs.macromol.7b01187
Macromolecules 2017, 50, 7657−7665

of the layers are 1.84×10^{-6} for PS, 3.63×10^{-6} for SiO_x, and 3.85×10^{-6} for Si at the X-ray energy.

Grazing incidence small-angle X-ray scattering (GISAXS) experiments were performed at the G1 beamline (CHESS). The measurements were taken using incident X-ray angles of 0.14°. The X-ray energy was 9.9 keV, at which the critical angle of PS is 0.12°.

Small-angle X-ray scattering (SAXS) was carried out on a solution of PS50k and Au nanoparticles (0.25 vol %) in toluene. The experiment was carried out on a Bruker Nanostar U at the Center for Functional Nanomaterials at Brookhaven National Laboratory, using the Cu Kα X-ray source. Fitting of the form factor of the spherical nanoparticles[76] resulted in a diameter of 2.8 nm for the gold nanoparticle (data not shown).

X-ray photoelectron spectroscopy (XPS) was performed using a UVH Technology UHV 7500 to characterize the PS/Au thin films and the residual layers left over after toluene rinsing the annealed film. The Al Kα X-ray source gave E_{exc} = 1486.61 eV. The emission angle of the photoelectrons was 45°, and the resulting sampling depth was 10 nm.

In order to quantify the role of the surface energies of the Si substrate, polymer, and nanoparticles on the mobility and dispersion or segregation of the nanoparticles, contact angle measurements were carried out on a monolayer of the Au nanoparticles. The layer was prepared by spin-coating a 0.05% solution of the Au nanoparticles in a toluene solution for 30 s at 2500 rpm on Si wafer cleaned by the method described above and dried the film. Static contact angle measurements with three liquids (water, 1,4-butanediol, and glycerol) were carried out using a CAM 200 optical contact angle meter (KSV Instruments, Ltd.) equipped with a video camera. A static contact angle (θ) of a film surface was determined on the basis of the three-phase contact line with a 2 μL liquid droplet. All the results were obtained by averaging data from at least five individual samples and 10 readings per sample at different locations. The data are summarized in the Supporting Information.

Specular neutron reflectivity (NR) measurements were performed on the NG-7 reflectometer at the National Institute of Standards and Technology, Center for Neutron Research. The wavelength (λ_N) of the neutron beams was 0.47 nm with $\Delta\lambda_N/\lambda_N$ = 2.5%. The bilayer samples were prepared by floating a layer of dPS on top of prepared hydrogenated PS flattened layer, which contained 0 or 0.25% Au nanoparticles. The bilayer samples were dried at 50 °C for 12 h before the NR experiments. The samples were then annealed at 150 °C in a vacuum oven for prescribed durations and then rapidly quenched rapidly to room temperature by placing on a cool metal block. The NR data corrected for the background scattering were analyzed by comparing the observed reflectivity curves with the calculated ones based on model SLD profiles with three fitting parameters for each layer: film thickness, SLD, and roughness between the layers represented as a Gaussian function.[77] To fit the NR data, we used a four-layer model: Si (SLD = 2.08×10^{-4} nm^{-2}), SiO_2 (SLD = 3.44×10^{-4} nm^{-2}), the hPS/Au flattened layer (SLD = 1.42×10^{-4} nm^{-2}), and the dPS overlayer (SLD = 6.0×10^{-4} nm^{-2}). The SLD profiles were subsequently converted into the corresponding polymer volume fraction profiles using the following equation:

$$SLD_{mix} = SLD_{dPS} \times \phi(z) + SLD_{hPS/Au} \times (1 - \phi(z)) \quad (1)$$

where $\phi(z)$ is the volume fraction of dPS at a distance z from the SiO_x layer. It is noted that the SLD profile at the adsorbed polymer−free polymer interface would be asymmetric due to a gradient of segmental diffusion. However, as shown in Figure S7, the symmetric SLD profiles could fit the NR data reasonably. This would be due to the fact that the interfacial width is relatively narrow such that the spatial resolution of the technique might not be sensitive enough to provide a unique solution regarding the shape of the sharp interface.

For the SFG experiments, quartz prisms were cleaned using a hot piranha solution for 30 min and subsequently rinsed with deionized water thoroughly. We previously confirmed that the cleaned quartz prism and the SiO_x/Si substrate showed very similar hydrophobicity and interaction with PS,[42] proving that the substrates have no significant effects on the resultant PS adsorbed layers prepared on the different solids. A PS/Au thin film (20 nm in thickness) was prepared by spin-coating the PS/Au/toluene solution onto the cleaned quartz with a rotation speed of 2500 rpm. The PS/Au thin film was postannealed at 150 °C under vacuum for 96 h to mimic the experimental conditions used for the dewetting experiments. In order to suppress any signals from the polymer/air interface,[52] the annealed PS/Au thin film was pressed together with another PS spin-cast film (200 nm in thickness) prepared independently on a quartz window. We confirmed that such a sandwich configuration does not affect the chain conformations at the polymer melt−solid interface.[42] Visible (wavelength of 532 nm) and tunable infrared (IR) beams were introduced from the quartz prism side with incident angles of 70° and 50°, respectively. The measurements with ssp (SFG/s; visible/s; and IR/p) combination were used to detect functional groups oriented only along the direction normal to the interface.[52]

■ ASSOCIATED CONTENT

Supporting Information

The Supporting Information is available free of charge on the ACS Publications website at DOI: 10.1021/acs.macromol.7b01187.

XPS results, additional AFM results, additional GISAXS and NR results, contact angle results, and calculations of surface energies (PDF)

■ AUTHOR INFORMATION

Corresponding Author

*E-mail tadanori.koga@stonybrook.edu (T.K.).

ORCID

Jonathan G. Rudick: 0000-0002-3769-1103
Tadanori Koga: 0000-0003-1316-6133
Keiji Tanaka: 0000-0003-0314-3843
Alamgir Karim: 0000-0003-1302-9374

Author Contributions

D.A.B. and N.J. contributed equally.

Funding

T.K. acknowledges financial support from the NSF (CMMI-1332499). A.K. acknowledges the W.M. Keck Foundation and the NSF (DMR-1411046) for their support related to this work.

Notes

The authors declare no competing financial interest.

■ ACKNOWLEDGMENTS

The Joint Photon Sciences Institute at Stony Brook University provided support for travel and subsistence to facilitate access to CHESS. This research used resources of the Center for Functional Nanomaterials, which is a U.S. DOE Office of Science Facility, at Brookhaven National Laboratory under Contract DE-SC0012704. CHESS is supported by the NSF & NIH/NIGMS via NSF Award DMR-1332208. The identification of any commercial product or trade name does not imply endorsement or recommendation by the NIST.

■ REFERENCES

(1) Sershen, S. R.; Westcott, S. L.; Halas, N. J.; West, J. L. Independent optically addressable nanoparticle-polymer optomechanical composites. *Appl. Phys. Lett.* **2002**, *80* (24), 4609−4611.

(2) Saunders, B. R.; Turner, M. L. Nanoparticle−polymer photovoltaic cells. *Adv. Colloid Interface Sci.* **2008**, *138* (1), 1−23.

(3) Bajaj, A.; Miranda, O. R.; Kim, I.-K.; Phillips, R. L.; Jerry, J.; Bunz, U. H. F.; Rotello, V. M. Detection and differentiation of normal, cancerous, and metastatic cells using nanoparticle-polymer sensor arrays. *Proc. Natl. Acad. Sci. U. S. A.* **2009**, *106* (27), 10912−10916.

DOI: 10.1021/acs.macromol.7b01187
Macromolecules 2017, 50, 7657−7665

(4) Jones, R. A.; Richards, R. W. *Polymers at Surfaces and Interfaces*; Cambridge University Press: 1999.
(5) Veinot, J. G. C.; Marks, T. J. Toward the ideal organic light-emitting diode. The versatility and utility of interfacial tailoring by cross-linked siloxane interlayers. *Acc. Chem. Res.* **2005**, *38* (8), 632−643.
(6) Dhar, P.; Khlyabich, P. P.; Burkhart, B.; Roberts, S. T.; Malyk, S.; Thompson, B. C.; Benderskii, A. V. Annealing-induced changes in the molecular orientation of poly-3-hexylthiophene at buried interfaces. *J. Phys. Chem. C* **2013**, *117* (29), 15213−15220.
(7) Barnes, K. A.; Karim, A.; Douglas, J. F.; Nakatani, A. I.; Gruell, H.; Amis, E. J. Suppression of dewetting in nanoparticle-filled polymer films. *Macromolecules* **2000**, *33* (11), 4177−4185.
(8) Mackay, M. E.; Hong, Y.; Jeong, M.; Hong, S.; Russell, T. P.; Hawker, C. J.; Vestberg, R.; Douglas, J. F. Influence of dendrimer additives on the dewetting of thin polystyrene films. *Langmuir* **2002**, *18* (5), 1877−1882.
(9) Wei, B.; Gurr, P. A.; Genzer, J.; Qiao, G. G.; Solomon, D. H.; Spontak, R. J. Dewetting of star nanogel/homopolymer blends from an immiscible homopolymer substrate. *Macromolecules* **2004**, *37*, 7857−7860.
(10) Besancon, B. M.; Green, P. F. Polystyrene-based single-walled carbon nanotube nanocomposite thin films: Dynamics of structural instabilities. *Macromolecules* **2005**, *38* (1), 110−115.
(11) Kropka, J. M.; Green, P. F. Control of interfacial instabilities in thin polymer films with the addition of a miscible component. *Macromolecules* **2006**, *39* (25), 8758−8762.
(12) Xavier, J. H.; Sharma, S.; Seo, Y. S.; Isseroff, R.; Koga, T.; White, H.; Ulman, A.; Shin, K.; Satija, S. K.; Sokolov, J.; Rafailovich, M. H. Effect of nanoscopic fillers on dewetting dynamics. *Macromolecules* **2006**, *39* (8), 2972−2980.
(13) Koo, J.; Shin, K.; Seo, Y. S.; Koga, T.; Park, S.; Satija, S. K.; Chen, X.; Yoon, K.; Hsiao, B. S.; Sokolov, J. C.; Rafailovich, M. H. Stabilizing thin film polymer bilayers against dewetting using multiwalled carbon nanotubes. *Macromolecules* **2007**, *40* (26), 9510−9516.
(14) McGarrity, E. S.; Frischknecht, A. L.; Frink, L. J. D.; Mackay, M. E. Surface-induced first-order transition in athermal polymer-nanoparticle blends. *Phys. Rev. Lett.* **2007**, *99* (23), 238302.
(15) Krishnan, R. S.; Mackay, M. E.; Duxbury, P. M.; Pastor, A.; Hawker, C. J.; Van Horn, B.; Asokan, S.; Wong, M. S. Self-assembled multilayers of nanocomponents. *Nano Lett.* **2007**, *7* (2), 484−489.
(16) Krishnan, R. S.; Mackay, M. E.; Duxbury, P. M.; Hawker, C. J.; Asokan, S.; Wong, M. S.; Goyette, R.; Thiyagarajan, P. Improved polymer thin-film wetting behavior through nanoparticle segregation to interfaces. *J. Phys.: Condens. Matter* **2007**, *19* (35), 356003.
(17) Holmes, M. A.; Mackay, M. E.; Giunta, R. K. Nanoparticles for dewetting suppression of thin polymer films used in chemical sensors. *J. Nanopart. Res.* **2007**, *9* (5), 753−763.
(18) Han, J. T.; Lee, G. W.; Kim, S.; Lee, H. J.; Douglas, J. F.; Karim, A. Direct observation of interfacial C_{60} cluster formation in polystyrene−C_{60} nanocomposite films. *Nanotechnology* **2009**, *20*, 105705.
(19) Mukherjee, R.; Das, S.; Das, A.; Sharma, S. K.; Raychaudhuri, A. K.; Sharma, A. Stability and dewetting of metal nanoparticle filled thin polymer films: Control of instability length scale and dynamics. *ACS Nano* **2010**, *4* (7), 3709−3724.
(20) Wong, H. C.; Cabral, J. T. Spinodal clustering in thin films of nanoparticle-polymer mixtures. *Phys. Rev. Lett.* **2010**, *105* (3), 038301.
(21) Chen, F.; Clough, A.; Reinhard, B. M.; Grinstaff, M. W.; Jiang, N.; Koga, T.; Tsui, O. K. C. Glass transition temperature of polymer−nanoparticle composites: Effect of polymer−particle interfacial energy. *Macromolecules* **2013**, *46* (11), 4663−4669.
(22) Roy, S.; Bandyopadhyay, D.; Karim, A.; Mukherjee, R. Interplay of substrate surface energy and nanoparticle concentration in suppressing polymer thin film dewetting. *Macromolecules* **2015**, *48* (2), 373−382.
(23) Bandyopadhyay, D.; Douglas, J. F.; Karim, A. Influence of C_{60} nanoparticles on the stability and morphology of miscible polymer blend films. *Macromolecules* **2011**, *44* (20), 8136−8142.
(24) Lee, J. Y.; Buxton, G. A.; Balazs, A. C. Using nanoparticles to create self-healing composites. *J. Chem. Phys.* **2004**, *121* (11), 5531−5539.
(25) Kropka, J. M.; Putz, K. W.; Pryamitsyn, V.; Ganesan, V.; Green, P. F. Origin of dynamical properties in pmma-C_{60} nanocomposites. *Macromolecules* **2007**, *40* (15), 5424−5432.
(26) Meli, L.; Arceo, A.; Green, P. F. Control of the entropic interactions and phase behavior of athermal nanoparticle/homopolymer thin film mixtures. *Soft Matter* **2009**, *5* (3), 533−537.
(27) Green, P. F. The structure of chain end-grafted nanoparticle/homopolymer nanocomposites. *Soft Matter* **2011**, *7* (18), 7914−7926.
(28) Jiang, N.; Wang, J.; Di, X.; Cheung, J.; Zeng, W.; Endoh, M. K.; Koga, T.; Satija, S. K. Nanoscale adsorbed structures as a robust approach for tailoring polymer film stability. *Soft Matter* **2016**, *12*, 1801−1809.
(29) Durning, C. J.; O'Shaughnessy, B.; Sawhney, U.; Nguyen, D.; Majewski, J.; Smith, G. S. Adsorption of poly(methyl methacrylate) melts on quartz. *Macromolecules* **1999**, *32* (20), 6772−6781.
(30) Fujii, Y.; Yang, Z. H.; Leach, J.; Atarashi, H.; Tanaka, K.; Tsui, O. K. C. Affinity of polystyrene films to hydrogen-passivated silicon and its relevance to the T_g of the films. *Macromolecules* **2009**, *42* (19), 7418−7422.
(31) Harton, S. E.; Kumar, S. K.; Yang, H. C.; Koga, T.; Hicks, K.; Lee, E.; Mijovic, J.; Liu, M.; Vallery, R. S.; Gidley, D. W. Immobilized polymer layers on spherical nanoparticles. *Macromolecules* **2010**, *43* (7), 3415−3421.
(32) Koga, T.; Jiang, N.; Gin, P.; Endoh, M.; Narayanan, S.; Lurio, L.; Sinha, S. K. Impact of an irreversibly adsorbed layer on local viscosity of nanoconfined polymer melts. *Phys. Rev. Lett.* **2011**, *107*, 225901.
(33) Rotella, C.; Napolitano, S.; Vandendriessche, S.; Valev, V. K.; Verbiest, T.; Larkowska, M.; Kucharski, S.; Wubbenhorst, M. Adsorption kinetics of ultrathin polymer films in the melt probed by dielectric spectroscopy and second-harmonic generation. *Langmuir* **2011**, *27* (22), 13533−13538.
(34) Napolitano, S.; Wubbenhorst, M. The lifetime of the deviations from bulk behaviour in polymers confined at the nanoscale. *Nat. Commun.* **2011**, *2*, 260−267.
(35) Gin, P.; Jiang, N. S.; Liang, C.; Taniguchi, T.; Akgun, B.; Satija, S. K.; Endoh, M. K.; Koga, T. Revealed architectures of adsorbed polymer chains at solid-polymer melt interfaces. *Phys. Rev. Lett.* **2012**, *109* (26), 265501.
(36) Jiang, N.; Shang, J.; Di, X.; Endoh, M. K.; Koga, T. Formation mechanism of high-density, flattened polymer nanolayers adsorbed on planar solids. *Macromolecules* **2014**, *47* (8), 2682−2689.
(37) Housmans, C.; Sferrazza, M.; Napolitano, S. Kinetics of irreversible chain adsorption. *Macromolecules* **2014**, *47* (10), 3390−3393.
(38) Jiang, N.; Sendogdular, L.; Di, X.; Sen, M.; Gin, P.; Endoh, M. K.; Koga, T.; Akgun, B.; Dimitriou, M.; Satija, S. Effect of CO_2 on a mobility gradient of polymer chains near an impenetrable solid. *Macromolecules* **2015**, *48* (6), 1795−1803.
(39) Bal, J. K.; Beuvier, T.; Beena Unni, A.; Chavez Panduro, E. A.; Vignaud, G.; Delorme, N.; Chebil, M. S.; Grohens, Y.; Gibaud, A. Stability of polymer ultrathin films (<7 nm) made by a top-down approach. *ACS Nano* **2015**, *9* (8), 8184−8193.
(40) Burroughs, M. J.; Napolitano, S.; Cangialosi, D.; Priestley, R. D. Direct measurement of glass transition temperature in exposed and buried adsorbed polymer nanolayers. *Macromolecules* **2016**, *49* (12), 4647−4655.
(41) Unni, A. B.; Vignaud, G.; Bal, J. K.; Delorme, N.; Beuvier, T.; Thomas, S.; Grohens, Y.; Gibaud, A. Solvent assisted rinsing: Stability/instability of ultrathin polymer residual layer. *Macromolecules* **2016**, *49* (5), 1807−1815.
(42) Sen, M.; Jiang, N.; Cheung, J.; Endoh, M. K.; Koga, T.; Kawaguchi, D.; Tanaka, K. Flattening process of polymer chains

DOI: 10.1021/acs.macromol.7b01187
Macromolecules 2017, 50, 7657−7665

irreversibly adsorbed on a solid. *ACS Macro Lett.* **2016**, *5* (4), 504−508.
(43) Carrillo, J.-M. Y.; Cheng, S.; Kumar, R.; Goswami, M.; Sokolov, A. P.; Sumpter, B. G. Untangling the effects of chain rigidity on the structure and dynamics of strongly adsorbed polymer melts. *Macromolecules* **2015**, *48* (12), 4207−4219.
(44) Johnson, H. E.; Granick, S. New Mechanism of Nonequilibrium Polymer Adsorption. *Science* **1992**, *255*, 966−968.
(45) Douglas, J. F.; Johnson, H. E.; Granick, S. A Simple Kinetic Model of Polymer Adsorption and Desorption. *Science* **1993**, *262*, 2010−2012.
(46) Guiselin, O. Irreversible adsorption of a concentrated polymer solution. *Europhys. Lett.* **1992**, *17* (3), 225−230.
(47) van Zanten, J. H.; Wallace, W. E.; Wu, W. -l. Effect of strongly favorable substrate interactions on the thermal properties of ultrathin polymer films. *Phys. Rev. E: Stat. Phys., Plasmas, Fluids, Relat. Interdiscip. Top.* **1996**, *53* (3), R2053−R2056.
(48) Linse, P.; Källrot, N. Polymer adsorption from bulk solution onto planar surfaces: Effect of polymer flexibility and surface attraction in good solvent. *Macromolecules* **2010**, *43* (4), 2054−2068.
(49) Chandran, S.; Begam, N.; Padmanabhan, V.; Basu, J. K. Confinement enhances dispersion in nanoparticle-polymer blend films. *Nat. Commun.* **2014**, *5*, 3697.
(50) Gautam, K. S.; Schwab, A. D.; Dhinojwala, A.; Zhang, D.; Dougal, S. M.; Yeganeh, M. S. Molecular structure of polystyrene at air/polymer and solid/polymer interfaces. *Phys. Rev. Lett.* **2000**, *85* (18), 3854−3857.
(51) Frank, C. W.; Rao, V.; Despotopoulou, M. M.; Pease, R. F. W.; Hinsberg, W. D.; Miller, R. D.; Rabolt, J. F. Structure in thin and ultrathin spin-cast polymer films. *Science* **1996**, *273* (5277), 912−915.
(52) Tsuruta, H.; Fujii, Y.; Kai, N.; Kataoka, H.; Ishizone, T.; Doi, M.; Morita, H.; Tanaka, K. Local conformation and relaxation of polystyrene at substrate interface. *Macromolecules* **2012**, *45* (11), 4643−4649.
(53) Calchera, A. R.; Curtis, A. D.; Patterson, J. E. Plasma treatment of polystyrene thin films affects more than the surface. *ACS Appl. Mater. Interfaces* **2012**, *4* (7), 3493−3499.
(54) Tatek, Y. B.; Tsige, M. Structural properties of atactic polystyrene adsorbed onto solid surfaces. *J. Chem. Phys.* **2011**, *135* (17), 174708.
(55) Kraus, J.; Müller-Buschbaum, P.; Kuhlmann, T.; Schubert, D. W.; Stamm, M. Confinement effects on the chain conformation in thin polymer films. *Europhys. Lett.* **2000**, *49* (2), 210−216.
(56) Luo, H.; Gersappe, D. Dewetting dynamics of nanofilled polymer thin films. *Macromolecules* **2004**, *37* (15), 5792−5799.
(57) Sharma, A. Many paths to dewetting of thin films: Anatomy and physiology of surface instability. *Eur. Phys. J. E: Soft Matter Biol. Phys.* **2003**, *12* (3), 397−408.
(58) Ferreira, P. G.; Ajdari, A.; Leibler, L. Scaling law for entropic effects at interfaces between grafted layers and polymer melts. *Macromolecules* **1998**, *31* (12), 3994−4003.
(59) Raphael, E.; De Gennes, P. G. Rubber adhesion with connector molecules. *J. Phys. Chem.* **1992**, *96*, 4002−4007.
(60) Reiter, G.; Sharma, A.; Casoli, A.; David, M.-O.; Khanna, R.; Auroy, P. Thin film instability induced by long-range forces. *Langmuir* **1999**, *15* (7), 2551−2558.
(61) Reiter, G.; Schultz, J.; Auroy, P.; Auvray, L. Improving adhesion via connector polymers to stabilize non-wetting liquid films. *Europhys. Lett.* **1996**, *33* (1), 29.
(62) Reiter, G.; Auroy, P.; Auvray, L. Instabilities of thin polymer films on layers of chemically identical grafted molecules. *Macromolecules* **1996**, *29* (6), 2150−2157.
(63) Kim, J. U.; O'Shaughnessy, B. Morphology selection of nanoparticle dispersions by polymer media. *Phys. Rev. Lett.* **2002**, *89*, 238301.
(64) Reiter, G. Mobility of polymers in films thinner than their unperturbed size. *Europhys. Lett.* **1993**, *23* (8), 579−584.
(65) Reiter, G. Dewetting of thin polymer-films. *Phys. Rev. Lett.* **1992**, *68* (1), 75−78.
(66) Lee, Y.; Loew, A.; Sun, S. Surface- and structure-dependent catalytic activity of Au nanoparticles for oxygen reduction reaction. *Chem. Mater.* **2010**, *22* (3), 755−761.
(67) Liu, Z.; Pappacena, K.; Cerise, J.; Kim, J.; Durning, C. J.; O'Shaughness, B.; Levicky, R. Organization of nanoparticles on soft polymer surfaces. *Nano Lett.* **2002**, *2* (3), 219−224.
(68) Lüttschwager, N. O.; Suhm, M. A. Stretching and folding of 2-nanometer hydrocarbon rods. *Soft Matter* **2014**, *10* (27), 4885−4901.
(69) Byrd, J. N.; Bartlett, R. J.; Montgomery, J. A., Jr. At what chain length do unbranched alkanes prefer folded conformations? *J. Phys. Chem. A* **2014**, *118* (9), 1706−1712.
(70) Koga, T.; Li, C.; Endoh, M. K.; Koo, J.; Rafailovich, M.; Narayanan, S.; Lee, D. R.; Lurio, L. B.; Sinha, S. K. Reduced viscosity of the free surface in entangled polymer melt films. *Phys. Rev. Lett.* **2010**, *104* (6), 066101.
(71) Jiang, N.; Endoh, M. K.; Koga, T. 'Marker' grazing-incidence x-ray photon correlation spectroscopy: A new tool to peer into the interfaces of nanoconfined polymer thin films. *Polym. J.* **2013**, *45* (1), 26−33.
(72) Kern, W. Cleaning solutions based on hydrogen peroxide for use in silicon semiconductor technology. *RCA Rev.* **1970**, *31*, 187−206.
(73) Müller-Buschbaum, P. Influence of surface cleaning on dewetting of thin polystyrene films. *Eur. Phys. J. E: Soft Matter Biol. Phys.* **2003**, *12* (3), 443−448.
(74) Koga, T.; Seo, Y.-S.; Jerome, J. L.; Ge, S.; Rafailovich, M. H.; Sokolov, J. C.; Chu, B.; Seeck, O. H.; Tolan, M.; Kolb, R. Low-density polymer thin film formation in supercritical carbon dioxide. *Appl. Phys. Lett.* **2003**, *83* (21), 4309−4311.
(75) Seeck, O. H.; Kaendler, I. D.; Tolan, M.; Shin, K.; Rafailovich, M. H.; Sokolov, J.; Kolb, R. Analysis of x-ray reflectivity data from low-contrast polymer bilayer systems using a Fourier method. *Appl. Phys. Lett.* **2000**, *76* (19), 2713−2715.
(76) Guinier, A.; Fournet, G. *Small-Angle Scattering of X-rays*; Wiley: 1955.
(77) Russell, T. P. X-ray and neutron reflectivity for the investigation of polymers. *Mater. Sci. Rep.* **1990**, *5* (4), 171−271.

DOI: 10.1021/acs.macromol.7b01187
Macromolecules 2017, 50, 7657−7665